

Identification of radiative characteristics of fused quartz containing bubbles using discrete ordinates method with Fresnel interfaces

by Dominique Baillis^(*), Harifidy Randrianalisoa^(*), Laurent Pilon^(**), Raymond Viskanta^(***)

^(*) Centre de Thermique de Lyon - UMR CNRS 5008 Institut National des Sciences Appliquées de Lyon 69621 - Villeurbanne Cedex - France. Email : domino@cethil.insa-lyon.fr

^(**) University of California, Los Angeles. Mechanical and Aerospace Engineering Department 37-132 Engineering IV - Box 951597 Los Angeles, CA 90095-1597 USA

^(***) Heat Transfer Laboratory, School of Mechanical Engineering, Purdue University, West Lafayette, IN 47907 USA

Abstract

Radiation characteristics of fused quartz containing bubbles (10 % porosity) are determined using inverse method based on theoretical and experimental bi-directional transmittances and reflectances. The Discrete Ordinates Method is used to solve the RTE. The internal and external interfaces are assumed to be optically smooth. The importance of the choice of the interpolation law has been shown, exponential law is appropriate in directions near the normal where there are large variations of intensity. The influence of thickness on the results are studied.

Nomenclature

g Henyey-Greenstein phase function parameter
 I_0 intensity of the collimated incident beam
 I spectral intensity of radiation
 ℓ_y sample thickness
 n real part of the complex index of refraction of the quartz continuous phase
 P phase function
 r_{12} reflectivity at the interface air-foam
 r_{21} reflectivity at the interface foam-air

T transmittance or reflectance

Greek symbols

β volumetric extinction coefficient

δ_{μ_i, μ_j} Kronecker's delta function
 $\delta_{\mu_i, \mu_j} = 1$ if $\mu_i = \mu_j$ and 0 otherwise
 κ volumetric absorption coefficient
 μ cosine of the polar angle
 θ angle defined between the incident and scattering direction
 θ_0 divergence angle of incident beam
 σ volumetric scattering coefficient
 ω volumetric scattering albedo coefficient

Subscripts

e experimental
 t theoretical
 λ monochromatic wavelength

1. Introduction

Foams and cellular materials bear practical importance in many applications. Examples range from food processes where foams can disrupt the process to space and building applications where they are used as insulating materials. In materials processing and manufacturing situations such as ceramics and glass manufacturing, gas bubbles can form in

the liquid and solid phases thus affecting the product quality. Thermal radiation in cellular materials is a predominant mode of energy transfer in most of these applications. Thus, the modeling of radiative transfer in cellular materials is of primary importance for the optimization of the performance of the engineering applications. An extensive review of radiative transfer in dispersed media was carried out by Viskanta and Mengüç in 1989 [1], and by Baillis and Sacadura in 2000 [2]. A porous medium is often treated as continuous, homogeneous, absorbing, and scattering medium. In order to evaluate the radiative heat transfer, radiation characteristics such as the extinction coefficient, the scattering albedo, and the single scattering phase function are required. They can be determined by different approaches :

- radiation characteristics can be predicted from porosity and bubble size distribution by considering a random arrangement of particles using for example Mie theory or geometric optics laws assuming independent scattering [3,4,5,6,7];
- Other methods consist of determining the radiation characteristics from a Monte Carlo approach at the local microscopic scale, taking into account the complex morphology of the porous medium [8, 9, 10, 11]
- Finally, other approaches are based on experimental measurements of reflectance and transmittance of the medium at macroscopic scale combined with an inverse method [12, 13, 14].

The present study is concerned with radiation characteristics of fused quartz containing bubbles (*figure 1*). Only a few studies have been reported on such media. Pilon and Viskanta [6] have studied the effect of volumetric void fraction and of the bubble size distribution on the radiation characteristics of semitransparent media containing gas bubbles using the model proposed by Fedorov and Viskanta [7] using the anomalous-diffraction approximation. Wong and Mengüç [11] used a ray-tracing method in a porous medium made of air spheres in a substrate to study the depolarization of radiation by the medium. Moreover the earlier model of water foam by Dombrovsky [15] can be also mentioned. The objective of this work is to determine the radiation characteristics of such media using an inverse method. Until now, studies have been concerned only with high porosity media (larger than 80 %) with negligible reflection at the interfaces. In this work the porosity is approximately 10 % and reflectivities must be accounted for in the model of the inverse method. The porosity being small, the effect of open bubbles at the interfaces is neglected and the surface is assumed to be optically smooth. Note that Wong and Mengüç [11] also treated surfaces were as optically smooth. Moreover in the study by Fedorov and Viskanta [7] the external surface reflectivity (r_{12}) between the air and the foam layer was also calculated assuming interfaces optically smooth using the Fresnel equations. However, due to the presence of scatterers (bubbles) in the foam layer, the radiation field inside the layer was assumed to be isotropic and the internal surface reflectivity r_{21} was calculated by considering a diffuse foam/air interface.

The present study focuses on the inverse method applied to cellular materials with small porosities. First, the inverse method using experimental and theoretical transmittance and reflectance is briefly described. Then the model used to calculate transmittances and reflectances, based on the Discrete Ordinates Method (DOM) to solve the RTE is described taking into account reflectivities at the interfaces. Due to the optically smooth interfaces with Fresnel equations, interpolation laws are used to calculate intensity in the directions of the quadrature. Finally results obtained for three samples with different thicknesses (3 mm, 5 mm, and 9.9 mm) are given. The influence of the different types of interpolations on the inversion results is studied. Moreover, the condition number indicating the ability of the inverse method to identify radiation characteristics is studied as a function of the sample thickness. The

comparison between experimental and theoretical transmittances and reflectances enables one to study the validity of the modeling of the boundary conditions at the interfaces.

2. Parameter identification method

The radiative characteristics of semitransparent media are the single scattering albedo ω , the extinction coefficient β and single scattering phase function P . The scattering phase function was assumed to follow the Henyey-Greenstein form involving the asymmetry factor g_λ and expressed as:

$$P_\lambda(\theta) = \frac{1 - g_\lambda^2}{(1 + g_\lambda^2 - 2g_\lambda \cos\theta)^{1.5}} \quad (1)$$

As a result, there are three unknown parameters: $(p_k)_{k=1,3} = (\omega, \beta, g)$

For a given sample, the parameter identification method used is based upon:

- the experimental data of bi-directional transmittances and reflectances (T_{ei}) obtained for several measurement directions (i),
- the theoretical bi-directional transmittances and reflectances (T_{ii}) calculated for the same directions than the ones of the experimental data

For each wavelength the goal is to determine the radiative parameters $(p_k)_{k=1,3} = (\omega, \beta, g)$, which minimize the quadratic relative differences (F) between the measured and calculated transmittances over the N measurements:

$$F(p_1, p_2, p_3) = \sum_{i=1}^N [T_{ii}(p_1, p_2, p_3) - T_{ei}]^2 \quad (2)$$

The transmittances or reflectances $T(\mu)$ for normal incidence are defined by the following expression:

$$T(\mu) = \frac{I(\mu)}{I_0 d\omega_0} \quad (3)$$

where I is the transmitted or reflected intensity and I_0 the intensity of the collimated beam normally incident onto the sample within a solid angle $d\omega_0$.

The method adopted to achieve this minimization is the Gauss linearization method [16] which minimizes F by setting to zero the derivatives with respect to each of the unknown parameters. As the system is non-linear, an iterative process is performed over m iterations:

$$\begin{bmatrix} \sum_{i=1}^N \left(\frac{\partial T_{ii}}{\partial p_1} \right)^2 & \sum_{i=1}^N \left(\frac{\partial T_{ii}}{\partial p_1} \right) \left(\frac{\partial T_{ii}}{\partial p_2} \right) & \sum_{i=1}^N \left(\frac{\partial T_{ii}}{\partial p_1} \right) \left(\frac{\partial T_{ii}}{\partial p_3} \right) \\ \sum_{i=1}^N \left(\frac{\partial T_{ii}}{\partial p_2} \right) \left(\frac{\partial T_{ii}}{\partial p_1} \right) & \sum_{i=1}^N \left(\frac{\partial T_{ii}}{\partial p_2} \right)^2 & \sum_{i=1}^N \left(\frac{\partial T_{ii}}{\partial p_2} \right) \left(\frac{\partial T_{ii}}{\partial p_3} \right) \\ \sum_{i=1}^N \left(\frac{\partial T_{ii}}{\partial p_3} \right) \left(\frac{\partial T_{ii}}{\partial p_1} \right) & \sum_{i=1}^N \left(\frac{\partial T_{ii}}{\partial p_3} \right) \left(\frac{\partial T_{ii}}{\partial p_2} \right) & \sum_{i=1}^N \left(\frac{\partial T_{ii}}{\partial p_3} \right)^2 \end{bmatrix}^m \begin{bmatrix} \Delta p_1 \\ \Delta p_2 \\ \Delta p_3 \end{bmatrix}^m = - \begin{bmatrix} \sum_{i=1}^N (T_{ii} - T_{ei}) \frac{\partial T_{ii}}{\partial p_1} \\ \sum_{i=1}^N (T_{ii} - T_{ei}) \frac{\partial T_{ii}}{\partial p_2} \\ \sum_{i=1}^N (T_{ii} - T_{ei}) \frac{\partial T_{ii}}{\partial p_3} \end{bmatrix}^m \quad (4)$$

The resolution of the system of equations (4) permits to obtain the parameter variation Δp_k^m to add to each parameter p_k^m for each iteration m . The converged solution is reached when $\Delta p_k^m < 10^{-3}$. The matrix on the left hand side consists of the products of the sensitivity

coefficients $\left(\frac{\partial T_{ii}}{\partial p_k}\right)$ calculated from the theoretical model. The condition number CN of this matrix (M) can be calculated from the following relation:

$$CN(M) = \|M^{-1}\| \|M\| \quad (5)$$

where $\|M\|$ is the norm of the matrix, calculated from the elements a_{ij} of the matrix as follows:

$$\|M\| = \max_{i=1,n} \sum_{j=1}^n a_{ij} \quad (6)$$

The condition number CN is always larger than one. The larger the condition number the worse ill-conditioned the system is and small changes in the measurements, result in very large changes in the solution vector (Δp_k); it is then difficult to simultaneously determine all the unknown parameters. A bad condition number occurs when at least two of the sensitivity coefficients are quasi-linearly interdependent or when at least one is very small or very large compared to the others. The analysis of sensitivity coefficients and condition number is a powerful tool for understanding the physical behavior of the problem and for studying the feasibility of simultaneous determination of the unknown parameters [17].

The experimental spectral bi-directional transmittance data are obtained from an experimental setup that includes a Fourier-transform infrared spectrometer (FTS 60 A, Bio-Rad Inc) [14, 18]. The radiation emitted by the source is modulated and the incident radiation is normal to the sample with a divergence of half-angle $\theta_0 = 1.27^\circ$.

3. Theoretical model

The theoretical spectral bi-directional transmittances and reflectances are computed by solving the RTE based on the following assumptions: the radiation transfer is assumed to be (i) one-dimensional, (ii) azimuthal symmetry prevails, (iii) the medium emission term can be disregarded thanks to the radiation modulation and the phase sensitive detection.

3.1 RTE and boundary conditions

With these conditions, the radiative transfer equation can be written as follows:

$$\mu \frac{\partial I_\lambda}{\partial y} + \beta_\lambda I_\lambda = \frac{\sigma_\lambda}{2} \int_{-1}^1 I_\lambda(y, \mu') P_\lambda(\mu', \mu) d\mu' \quad (7)$$

The boundary conditions are obtained by assuming that the interfaces are optically smooth, i.e., surface roughness is small compared with the wavelength of radiation and reflections are specular. Moreover, the void fraction is small and the effect of open bubbles at the sample surface is neglected. Then, the boundary conditions associated with the RTE for normal incident radiation are the following:

$$I_\lambda(0, \mu) = r_{21} I_\lambda(0, -\mu) + \left(n_\lambda\right)^2 (1 - r_{12}) \delta_{\mu_0, \mu} I_\lambda(0, \mu_0) \quad \mu > 0 \quad (8)$$

$$I_\lambda(\ell_y, \mu) = r_{21} I_\lambda(\ell_y, -\mu) \quad \mu < 0 \quad (9)$$

where r_{12} and r_{21} are the interfacial reflectivities at the air/foam foam/air interfaces, respectively. The Kronecker's delta function is denoted $\delta_{\mu_0, \mu}$ ($=1$ if $\mu = \mu_0$ and $=0$ otherwise) with $\mu = \cos(\theta)$ and $\mu_0 = 1$ in the case of normal incidence.

When the absorption index is negligible the reflectivities are determined entirely from the refractive index n_λ [19]. This is the case for fused quartz in the spectral range of interest from

1.67 to 4.76 μm . The external reflectivity (r_{12}) can be calculated by the Fresnel's law of reflection. In the case of normal incident radiation it simplifies to [19]:

$$r_{12} = \frac{(n_{\lambda} - 1)^2}{(n_{\lambda} + 1)^2} \quad (10)$$

Due to the presence of a large number of scatterers (bubbles) in the condensed phase, the radiation field inside the layer does not reach the face normally. Thus the internal surface reflectivity r_{21} is given by [19]:

$$r_{21} = \frac{1}{2} \left[\frac{\sin^2(\theta - \chi)}{\sin^2(\theta + \chi)} + \frac{\text{tg}^2(\theta - \chi)}{\text{tg}^2(\theta + \chi)} \right] \quad (11)$$

where χ is the angle of incidence of the radiation from within the layer onto the surface of the slab and θ is the refraction angle at the interface. The angles χ and θ are defined by Snell's law: $n_{\lambda} \sin \chi = \sin \theta$

3.2 Method of solution of the RTE

The discrete ordinates method with a quadrature over 24 directions is applied to solve the integro-differential radiative transfer equation (Eq. 7). The quadrature used is a combination of two Gaussian quadratures and allows a concentration of ordinates in the neighborhood of the incident direction suitable for forward scattering materials. The spherical space is discretized into 12 directions for the positive range of μ and 12 other symmetric directions for the negative μ . More details about this quadrature can be found in Ref. [18]. By writing the radiative transfer equation (Eq.7) for each direction of the quadrature and by replacing the integral term by a sum over the 24 directions of the quadrature, a system of partial differential equations is obtained. Previous studies [14, 18] neglected reflection at the interfaces by virtue of the fact that porosity was fairly large. Thus, a simpler system of equations could be solved analytically by separating collimated radiation and scattered radiation. In the present study, the space is discretized in order to solve numerically the above system of partial differential equations with the associated boundary conditions [Equations (7) to (9)] by the control volume method. A linear scheme (diamond) is employed to evaluate the radiative intensity in the control volume [20]. For a number of control volumes larger than 190 the numerical results were shown to be independent of the number of control volumes.

3.3 Transmitted and reflected intensity calculations

The transmitted and reflected intensities leaving the sample and used to calculate transmittance and reflectance required in the inverse procedure (Eq. 4), take into account reflectivities and refraction at the interfaces. They are the following:

$$I_{\lambda}(0, \mu) = \eta_2 \delta_{\mu_0, \mu_j} I_{\lambda}(0, -\mu) + \left(\frac{1}{n_{\lambda}} \right)^2 (1 - r_{21}) I_{\lambda}(0, \mu_i) \quad \mu_j < 0 \quad (12)$$

$$I_{\lambda}(L, \mu) = \left(\frac{1}{n_{\lambda}} \right)^2 (1 - r_{21}) I_{\lambda}(L, \mu_i) \quad \mu_j > 0 \quad (13)$$

where μ_i correspond to the direction of the quadrature and μ correspond to the refraction angle defined by Snell's law $n_{\lambda} \sin \mu_i = \sin \mu$

In general, the direction μ is not a direction in the quadrature, except the directions $\mu = \pm 1$. Moreover, the direction μ depends on the wavelength. To circumvent this difficulty, interpolation is used to approximate the intensity in the quadrature directions. Different interpolation laws such as linear and exponential laws are tested their influence on the results is studied.

4. Results

4.1 Data

Three samples of different thicknesses (3, 5, and 9.9 mm) are studied, all having an average void fraction of 9.4%. Larger thickness has not been measured due to the assumption of one dimensional radiative transfer in the medium which could be no longer valid. *Figure 1* shows a photograph of a typical sample. The average bubble radius is $\bar{r} = 1.14$ mm. As one can see in *figure 1*, the bubbles are spherical in shape and randomly distributed. Radiation characteristics are identified for 337 different wavelengths in the spectral region from 1.67 μm to 4.76 μm . The sample thickness and the real part of the fused quartz complex index of refraction n_λ are required as input data in the identification process. Over the spectral range from 0.21 to 3.71 μm at 20°C, Malitson [21] fitted experimental data with the following three-term Sellmeier equation,

$$n_\lambda^2 = 1 - \frac{0.6961663\lambda^2}{\lambda^2 - (0.0684043)^2} + \frac{0.4079426\lambda^2}{\lambda^2 - (0.1162414)^2} + \frac{0.8974794\lambda^2}{\lambda^2 - (9.896161)^2} \quad (14)$$

Finally, due to the lack of energy in directions far from the normal direction of the sample only eight forward directions and three backward directions have been used in the inverse method.

4.2 Transmittances and reflectances-Influence of interpolation laws

As discussed in part 3, transmittances and reflectances leaving the sample are calculated for quadrature directions using interpolation laws. The variations of intensity are very important in directions near the normal direction. Three different intensity variation laws are tested: (1) linear variation law for all direction intervals, (2) exponential variation law for all direction intervals, and (3) exponential law to calculate intensity for the two forward directions nearest to the normal ($\theta=1.85^\circ$ and: 3.32°) and the two backward directions nearest to the normal ($\theta=178^\circ$ and 176°), where there is great variation of intensity, and linear variation to calculate intensity in the others directions. Experimental transmittances and reflectances are compared with theoretical results obtained from inverse method using these different laws. The results are similar for the three different sample thicknesses. For example, *figure 2* shows the results obtained for the 5 mm thick sample. The transmittance and reflectance are defined as the ratio of the energy transmitted or reflected by the incident energy. It can be observed that even if the three first directions are very close to each other there is great influence of the choice of the interpolation laws to calculate intensity in these directions due to the great intensity variations. The exponential law is more appropriate to calculate intensity in the two forward and backward directions nearest to the normal direction, It induces smallest deviations between experimental and theoretical transmittance and reflectance. For the intensity calculation in the other directions an exponential law as well as a linear law can be chosen, it has not great importance. It can be noticed that in the backward normal direction ($\theta=180^\circ$) deviation remains large. This deviation can be due to the uncertainty on the refraction index (n_λ) value. Indeed the influence of n_λ on reflectance in the normal direction is very significant and a small variation of n_λ induces a high variation on the reflectance.

Remarks:

- The cubic spline interpolation, used by Liou and Wu [22] to calculate radiative transfer in a multi-layer medium with Fresnel interfaces, has been also tested to approximate the angular distribution of intensity. This interpolation is not appropriate in this case due to the high variation of intensity in directions near the normal direction where it induces negative intensity values.
- The great variation of transmittance observed in the directions near the normal direction and the anisotropic behavior tends to confirm that internal surface reflectivity r_{21} should not be calculated considering a diffuse foam/air interface as assumed by Fedorov and Viskanta [7].

4.3 Radiative characteristics

Radiative characteristics retrieved by inverse method for three samples of different thickness are shown in *figure 3*. Only results for the case of exponential interpolation law are shown, but calculations have shown that deviation between results obtained from exponential interpolation law and exponential-linear law remains weak, less than 2.5 %. The extinction coefficient presents a peak around wavelength of 2.7 μm , it is attributed to hydroxyl groups present as impurities in the fused quartz. It can be observed that the Henyey-Greenstein parameter remains nearly the same for the three sample thicknesses. In contrast, extinction coefficient and single scattering albedo are significantly larger for the 3 mm thick sample than for the 5 and 9.9 mm thick samples. Moreover for 5 and 9.9 mm, results are similar although they are more oscillations for 5 mm thickness. Consequently, results for 3 mm thick sample should be considered with caution. In that case, the sample may be too thin to be treated as homogeneous. Deviation could also be attributed to the fact that the effect of open bubbles at the sample surface is no longer negligible, i.e., interfaces cannot be treated as optically smooth. Moreover it has been verified that the uncertainty on the refraction index value is not responsible for this deviation. Indeed, similar deviations have been observed using different refraction indices. As discussed before, if the condition number is too large there could be significant uncertainties on the results. Therefore the values of the condition number are studied.

4.4 Condition number

Figure 3 shows the condition number calculated for the three sample thicknesses based on the radiation characteristics determined by inverse method. The condition number varies greatly as a function of the sample thickness and wavelengths (*figure 4*). It is more appropriate for the 9.9 mm thick sample (it is less than 5×10^4), for the two other sample thickness it is higher reaching 10^7 for wavelengths less than 1.8 μm . *Figures 3 and 4* indicate that larger Henyey-Greenstein parameter induces significantly larger condition number. For wavelengths larger than 2.7 μm , the condition number is satisfactory for the three samples. Moreover the bad condition number cannot explain the large values of the extinction coefficient and of the single scattering albedo obtained for the 3 mm thick sample at all wavelengths.

4. Conclusion

Recently, radiation characteristics of porous medium containing gas bubbles have been predicted using anomalous-diffraction [6] or using a ray-tracing method [10, 11]. In this work the determination of radiation characteristics of such media using inverse method is studied. Until now, radiation characteristics identification method from bi-directional transmittance and reflectance have been used only for high porosity media (larger than 80 %) with no reflectivity at the interface. In the present study, the porosity is around of 10 % and reflectivities at the interfaces are modeled in the radiative model of the inverse method. The

internal and external interfaces are assumed to be optically smooth with specular reflections. The effect of open bubbles at the sample surface is neglected.

The Discrete Ordinates Method is used to solve the RTE. Due to the refraction at the interfaces the transmittances and reflectances in the quadrature directions are approached using interpolation laws. Even if directions near the normal are very close, the importance of the choice of the interpolation law has been shown, exponential law is more appropriate in directions near the normal where there are large variations of intensity.

The great variation of transmittance observed in the directions near the normal and the non isotropic compartment tends to confirm that internal surface reflectivity cannot be calculated considering a diffuse foam/air interface

The study of the condition number shows the great influence of Henyey-Greenstein parameter on the condition number.

Some limits of the model have been shown. Indeed if for 5 mm and 9.9 mm sample thickness, identified radiative parameters are close and tend to show that the model is correct, the case of 3 mm sample thickness tend to over-estimate extinction and albedo values. The 3 mm sample thickness could be too thin to be treated as homogeneous. Deviation could be also attributed to the fact that the effect of open bubbles at the sample surface have been neglected assuming that the interfaces are optically smooth. Such an assumption could be not valid for small thickness.

In the future it will be interesting for a theoretical model to predict the spectral radiation characteristics of fused quartz containing gas bubbles and compare them with experimental data.

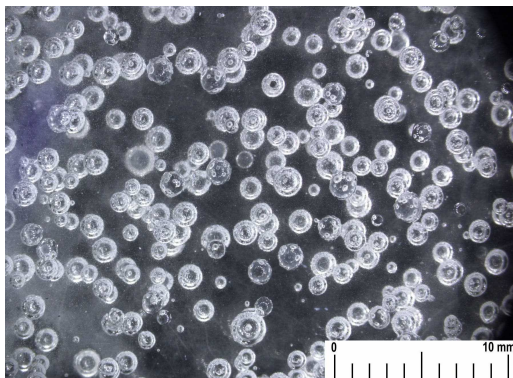


Figure 1 Photograph of a fused quartz sample containing bubbles

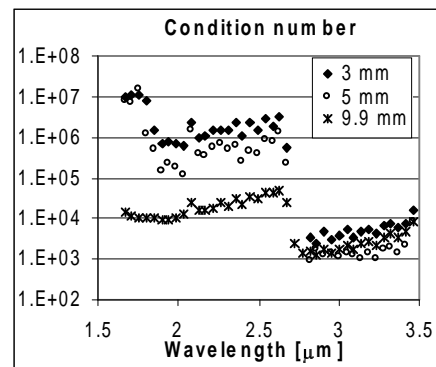


Figure 4 Condition number for the three sample thickness

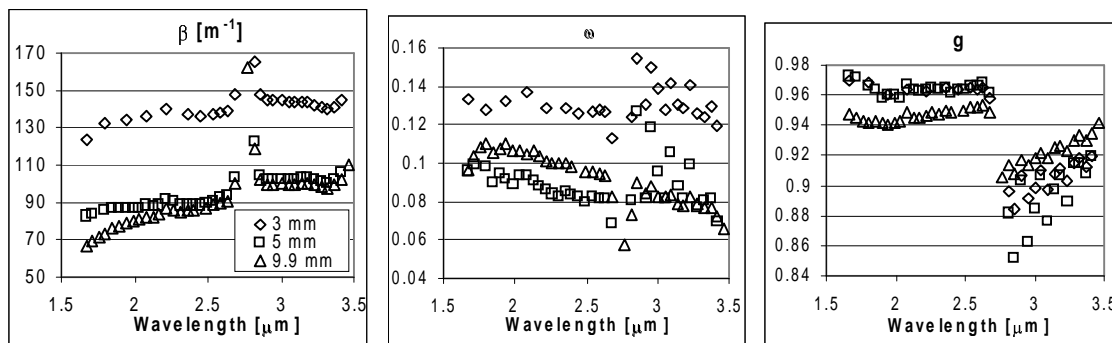


Figure 3 Radiation characteristics of the three sample thickness

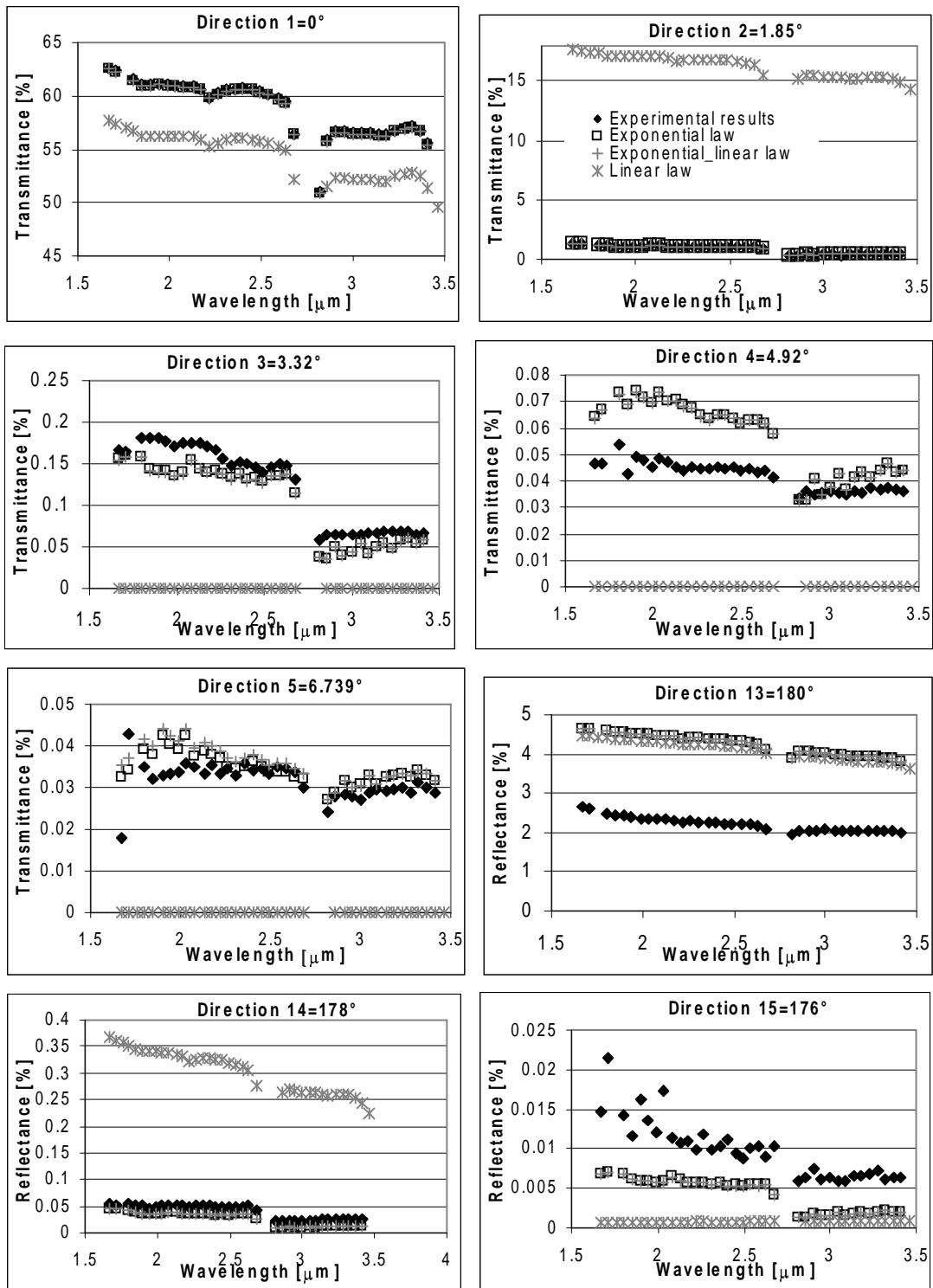


Figure 2. Experimental and theoretical transmittance and reflectance calculated using the three different types of interpolations (5 mm thick sample).

REFERENCES

- [1] VISKANTA, R., MENGUC P. (1989) *Radiative transfer in dispersed media*, Applied Mechanics Review, Vol. 42, N°. 9, pp. 241-259.

- [2] BAILLIS, D., SACADURA, J.F. (2000) *Thermal radiation properties of dispersed media : theoretical prediction and experimental characterization*, Journal of Quantitative Spectroscopy and Radiative Transfer, Vol. 67, pp. 327-363.
- [3] GLICKSMAN, L. R. (1992) *Radiation heat transfer in cellular foam insulation*, Developments in Radiative Heat Transfer, Heat Transfer Div., American Society of Mechanical Engineers, Vol. 203, pp. 45-54.
- [4] KUHN, J., EBERT, H. P., ARDUINI-CHUSTER, M. C., BÜTTNER, D., AND FRICKE, J., (1992) *Thermal transfer in polystyrene and polyurethane foam insulations*, International Journal of Heat and Mass Transfer, Vol. 35, N° 7, pp. 1795-1801.
- [5] DOERMANN, D., SACADURA J. F. (1996) *Heat transfer in open cell foam insulation*, Journal of Heat Transfer, Vol. 118, N° 1, pp. 88-93.
- [6] PILON, L., VISKANTA R. (2002) *Apparent radiation characteristics of semitransparent media containing gas bubbles*, twelfth International Heat Transfer Conference, Vol. 1, pp. 645-650.
- [7] FEDOROV A. G., VISKANTA R. (2000) *Radiation characteristics of glass foams*, Journal of the American Ceramic Society, Vol. 83, N° 11, pp. 2769-2776.
- [8] ARGENTO, C., BOUVARD D. (1996), A ray tracing method for evaluating the radiative heat transfer in porous media. Int. J. Heat Mass Transf. 39 (15), pp. 3175-3180.
- [9] ROZENBAUM, DE SOUZA MENEDED, ECHEGUT, AND LEVITZ (2000) ROZENBAUM, O., DE SOUSA MENESES, D., ECHEGUT, P. AND LEVITZ P. *Influence of the texture on the radiative properties of semitransparent materials*. Comparison between model and experiment. High Temp. High Press. 32 (1), pp. 61-66.
- [10] TANCREZ M. , TAINÉ J. (2002) *Characterization of the radiative properties of porous media with diffuse isotropic reflecting interfaces*, twelfth International Heat Transfer Conference, Vol. 1, pp. 627-632.
- [11] WONG B. T., MENGÜÇ M. P. (2002) *Depolarization of radiation by non-absorbing foams*, Journal of Quantitative Spectroscopy & Radiative Transfer 73, pp. 273-284.
- [12] HALE M., BOHN M. (1992) *Measurement of the radiative transport properties of reticulated alumina foams*. ASME/ASES Joint Solar Energy Conf. Paper 92-v-842
- [13] HENDRICKS, T, HOWELL J. (1996) *Absorption/scattering coefficients and scattering phase function in reticulated porous ceramics*. J. Heat Transfer Vol. 118, N° 1, pp. 79-87.
- [14] BAILLIS D., SACADURA J. F. (2002) *Identification of polyurethane foam radiative properties-Influence of Transmittance Measurements number* Journal of Thermophysics and Heat Transfer, Vol. 16, Number 2, pp. 200-206.
- [15] DOMBROVSKY L. A., *Radiation heat transfer in disperse systems*. Begel House, New York, 1996.
- [16] BECK, J. V., ARNOLD, K J., (1977), *Parameter estimation in engineering and science*, Wiley, New York, Chap. 7.
- [17] RAYNAUD M. (1999) *Strategy for experimental design and the estimation of parameters*, High Temperatures-High Pressures, N° 31, pp. 1-15.
- [18] NICOLAU, V.P, RAYNAUD, M., SACADURA, J. F. (1994) *Spectral radiative properties identification of fiber insulating materials*, International Journal of Heat and Mass Transfer, Vol. 37, Suppl. N° 1, pp. 311-324.
- [19] HOTTEL H. C., SAROFIM A. F. *Radiative transfer* (1967) McGraw-Hill, New York p. 129 Chapter 4.
- [20] DOERMANN D., *Modélisation des transferts thermiques dans des matériaux semi-transparents de type mousse à pores ouverts et prédiction des propriétés radiatives*, (1995), PhD thesis, Institut National des Sciences Appliquées de Lyon, France.
- [21] MALITSON I. H., *Interspecimen comparison of the refractive index of fused silica*, (1965) Journal of the Optical Society of America, Vol. 55, N° 10, pp. 1205-1209.
- [22] LIOU B. T., WU C. Y., (1996) *Radiative transfer in a multi-layer medium with Fresnel interfaces*, Journal of Heat and Mass Transfer, Vol. 32, pp. 103-107.